

## Molecular-dynamics simulations of premelting processes in $\text{Cr}_2\text{O}_3$

Miguel Angel San Miguel Barrera\* and Javier Fernández Sanz  
 Departamento de Química Física, Facultad de Química, E-41012, Sevilla, Spain

Luis Javier Álvarez

Laboratorio de Simulación de Materiales, Dirección General de Servicios de Cómputo Académico, Universidad Nacional Autónoma de México, Insurgentes Sur No. 3000, Zona Cultural, Ciudad Universitaria, Coyoacán 04510, México D. F., Mexico

José Antonio Odriozola

Departamento de Química Inorgánica e Instituto de Ciencia de Materiales, Universidad de Sevilla—CSIC, E-41012 Sevilla, Spain  
 (Received 15 December 1997; revised manuscript received 4 June 1998)

Molecular-dynamics simulations of the (0001) surface of  $\text{Cr}_2\text{O}_3$  were carried out in the [300–2800 K] range of temperatures using a classical Pauling-type pair potential. The analysis of the structural data shows a strong surface relaxation in agreement with experiment. Both static and dynamic surface properties indicate that a surface melting process occurs well below the melting point, which is estimated to be about 2500 K, in excellent agreement with the experimental value of 2556 K. The diffusive properties of this disordered phase are described and it is found that the main mechanism for diffusion involves hopping of surface atoms. [S0163-1829(98)08134-X]

### I. INTRODUCTION

Chromium oxide layers formed on the surface of stainless steel play an important role in preventing corrosion. At high temperatures, above 1000 K, cationic and anionic diffusion through the oxide layer results in a variety of mixed oxides containing chromium. The stability of these oxides is intimately related to the resistance of the material to corrosion at high temperature. One interesting aspect of chromium oxide that may shine some light on the role it plays as a coating is the crystal growth and the melting processes it undergoes as a function of temperature, and related to this, the point at which diffusion processes occur.

Recently, interest in a variety of processes in metal oxides has grown rapidly. Several studies on the melting of  $\text{MgO}$  have been published during the last few years<sup>1</sup> in which considerable attention has been paid to premelting processes. Among them, one of the most interesting involves a surface melting in which a thin liquidlike film below the melting temperature appears. The atoms in this film present intermediate dynamic behavior between solid and liquid phases. This is the reason why this partially molten phase is often called “quasiliquid.” Another type of disorder is that called roughening transition, which occurs when new structures are formed at the surface, such as steps, kinks, or ledges.<sup>2,3</sup>

The disordering and melting processes of rare-gas solids have been described by Lennard-Jones pair potentials.<sup>4</sup> Metals have been studied employing molecular-dynamics (MD) techniques in combination with some other formalism. For example, Chen, Barnett, and Landman<sup>5</sup> studied the disordering and melting of the surface of  $\text{Ni}(110)$  using MD simulations and the embedded-atom method, which is more appropriate to describe the interatomic interactions in metals than the pair potentials with conventional mathematical formulas.  $\text{Al}(110)$  and the low-index faces of copper have been studied

by means of the effective-medium theory,<sup>6</sup> and  $\text{Au}(111)$  using the “glue model.”<sup>7</sup>

To date some theoretical studies have been carried out on  $\text{Cr}_2\text{O}_3$  using molecular-mechanics methods,<sup>8</sup> however, only the static properties of the system are determined. In this work we examine the stability of chromium oxide as a function of increasing temperature through molecular-dynamics simulations. We report on an observed premelting process at the surface of simulated  $\text{Cr}_2\text{O}_3$  using a classical pairwise interaction potential. The diffusion coefficients and motion mechanism for ions of this premelted phase have also been investigated.

### II. METHOD

The molecular-dynamics method involves the solution of the classical equations of motion of  $N$  particles in a box with periodic boundaries, interacting according to a potential law. In order to explore the transferability of interaction potentials, two different forms have been used in our simulations. The first one is a Pauling-type function given by

$$V(r_{ij}) = \frac{q_i q_j e^2}{r_{ij}} + \frac{e^2}{n(\sigma_i + \sigma_j)} \left( \frac{\sigma_i + \sigma_j}{r_{ij}} \right)^n,$$

where  $q_i$  are the effective charges and  $\sigma_i$  are the atomic radii. The charges were taken from Cati *et al.*<sup>9</sup> and the radii from Shannon and Prewitt.<sup>10</sup> The exponent was taken to be 9 according to Adams and McDonald.<sup>11</sup> The long-range Coulombic forces were calculated using the Ewald summation method and a cutoff radius of 9.4 Å was used.

The second one has the same Coulombic term, plus a Buckingham-type short-range term of the form

$$V(r_{ij}) = \frac{q_i q_j e^2}{r_{ij}} + A_{ij} \exp\left(\frac{-r_{ij}}{\rho_{ij}}\right) - \frac{C_{ij}}{r_{ij}^6},$$

TABLE I. Pauling-type potential parameters.

Pauling			
Atom	Charge ( $e$ )	Radius ( $\text{\AA}$ )	
Cr	2.325	0.755	
O	-1.55	1.24	
Buckingham			
Pair	A (eV)	$\rho$ ( $\text{\AA}$ )	C (eV $\text{\AA}^6$ )
Cr-O	1734.1	0.3010	0.0
O-O	22764.3	0.1490	27.88

where  $q_i$  in this case are the formal charges of +3 and -2, and the values of parameters  $A$ ,  $\rho$ , and  $C$  were taken from Ref. 12. We used only the rigid-ion part of the potential. Although initially it included the electronic polarizability employing the shell model, it has been suggested that polarization effects accounted for using the shell model are negligible in some melting processes.<sup>13,14</sup> The parameters for both potentials are summarized in Table I.

The molecular-dynamics simulations were performed in the microcanonical ensemble using the SIMULA computer code.<sup>15</sup> The system consisted of 960 particles of which 384 represented chromium atoms and 576 oxygen atoms arranged in a hexagonal cell with  $a=b=19.803 \text{ \AA}$ ,  $c=27.131 \text{ \AA}$ ,  $\alpha=\beta=90^\circ$ , and  $\gamma=120^\circ$ . In order to simulate an infinite crystal, periodic boundary conditions were established for the hexagonal cell in the three directions. However, to simulate free surfaces of  $\text{Cr}_2\text{O}_3$  we used a slab formed by planes of atoms perpendicular to the basal direction. Separations of  $100 \text{ \AA}$  between the slabs in the basal direction were introduced in order to have independent slabs in the periodic system upon imposing boundary conditions. The integration of Newton's equations of motion was carried out using the standard leap-frog algorithm with an integration time step of  $10^{-15} \text{ s}$  and the periodic boundary conditions were handled using the standard minimal image method.<sup>16</sup> The conservation of energy was better than 1 in 10 000.

In order to obtain an equilibrated preheated sample, the system was taken from room temperature up to 1800 K in steps of 200 K through 5 ps thermalization runs in which the velocities were rescaled. From 1800 to 3000 K the simulations were carried out according to the following heating schedule: 30 ps of thermalization, 10 ps to verify if the system reached equilibrium, and 100 ps for statistics. In this range, the temperature was increased by steps of 100 K.

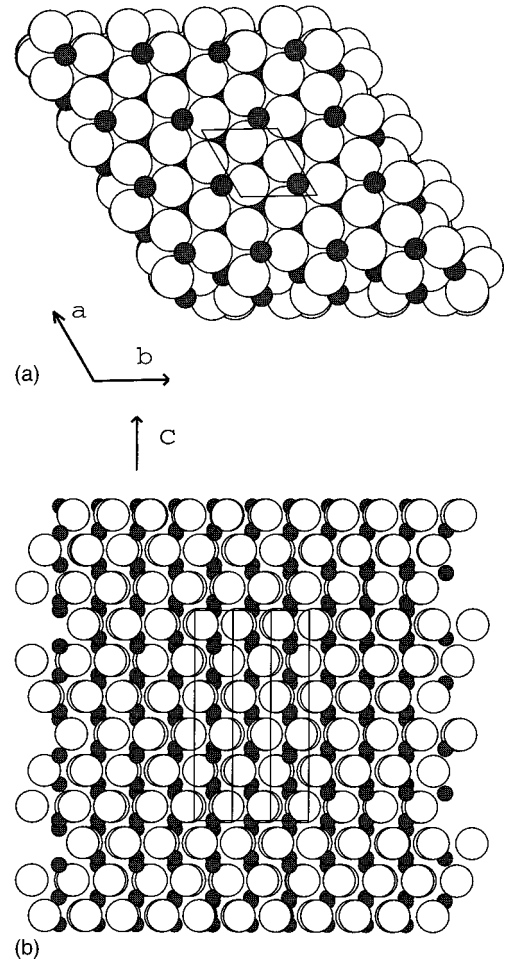


FIG. 1. (a) Top view of the starting configuration; (b) a side view. Note the chromium termination. Chromium atoms are represented by black balls.

### III. RESULTS AND DISCUSSION

Chromium oxide has a hexagonal closed packed structure of anions with two thirds of octahedral sites occupied by cations. Figure 1(a) shows a top view of the starting configuration, and Fig. 1(b) a side view. This configuration has a chromium termination, as can be seen from the figure where chromium atoms are represented by black balls. At the beginning of the simulation schedule a strong vertical relaxation was observed in agreement with experimental low-energy electron diffraction data.<sup>17</sup> Table II shows the distances from the surface of the outermost stacking layers of  $\text{Cr}_2\text{O}_3$  reported from experimental data, periodic Hartree-

TABLE II. Distances ( $\text{\AA}$ ) from the surface of the outermost stacking layers of  $\text{Cr}_2\text{O}_3$ .

Layer	Bulk structure	Experimental data <sup>a</sup>	HF calculation	Pauling	Buckingham
Cr	0.00	0.00	0.00	0.00	0.00
O	0.87	$0.58 \pm 0.04$	0.45	0.50	0.45
Cr	1.75	$1.32 \pm 0.06$	1.38	1.48	1.26
Cr	2.26	$1.61 \pm 0.15$	1.85	1.72	1.62
O	3.14	$2.65 \pm 0.08$	2.75	2.80	2.58

<sup>a</sup>Reference 17.

TABLE III. Surface energies in  $\text{J}/\text{m}^2$ .

	Hartree-Fock <sup>a</sup>	MM <sup>b</sup>	Pauling	Buckingham
Initial	9.3	4.6	4.0	5.2
Relaxed	3.1	1.6	1.7	3.4

<sup>a</sup>Reference 18.<sup>b</sup>Reference 8.

Fock calculations,<sup>18</sup> and our simulations. As can be seen from the table both potentials used in the present work give very similar results with displacements in agreement with the experiment. Surface energies estimated from periodic Hartree-Fock, molecular mechanics,<sup>8</sup> and our simulations are compared in Table III. The strong surface relaxation implies a large stabilization of the surface. In our calculations the energy diminishes more than twice when the system evolves from the original configuration to the relaxed one. This energy ratio is of the same order as those for the other two estimations.

In the course of the simulations we found that, even though the structural properties of the system computed either with one interaction potential or the other are very similar, the dynamic properties are not in agreement with known properties of the real material. In particular, the Buckingham potential model gives a melting point at 3400 K whereas the experimental value is 2556 K. As we will show below, the Pauling-type potential gives a value of 2500 K, therefore, from this point on we describe only the results obtained with the latter.

In Fig. 2, the total energy of the system computed at several temperatures in the range 1800–3000 K is reported. As can be seen the energy grows linearly up to 2450 K, where a discontinuity is observed. This linear behavior continues for temperatures higher than 2550 K and is typical of the heating of a homogeneous phase. The most outstanding feature of this plot is the discontinuity observed at  $\sim 2500$  K indicating a first-order phase transition corresponding to the melting of the system. This temperature is in good agreement with the experimental melting point of 2556 K, the error being of 0.02%.

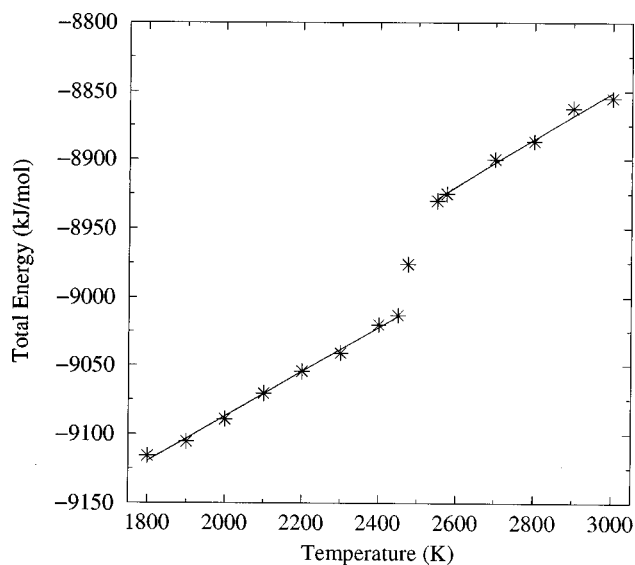


FIG. 2. Total energy of the system versus temperature.

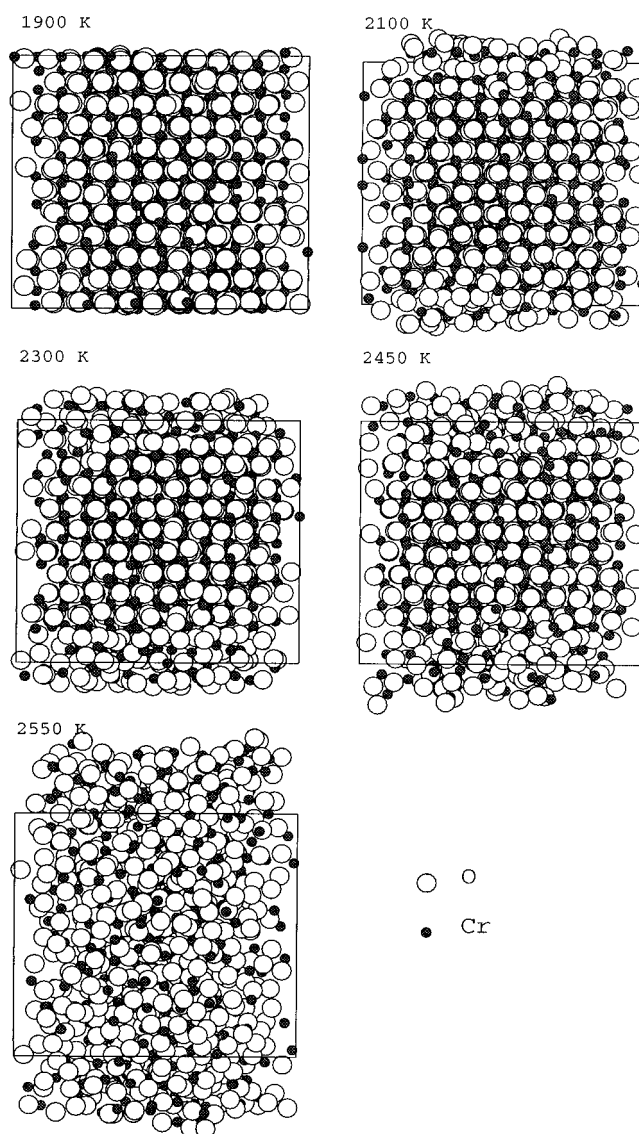


FIG. 3. Snapshots of the system between 1900 and 2550 K.

Figure 3 shows five snapshots of the system between 1900 and 2550 K. In the first case an orderly system can still be observed. On increasing temperature, the inner layers keep their bulk structure up to 2450 K, however, the outermost layers disorder according to a surface melting process. Beyond 2550 K, the order is completely lost, and the material is melted.

The premelting process can be monitored by analyzing the total density profiles of the system along the  $c$  axis reported in Fig. 4. In the 300–1900 K range, the profiles exhibit well-resolved peaks according to a crystalline solid. Upon heating, the profiles for the outermost shells broaden, reflecting the appearance of surface disorder, while the inner region preserves its structure up to 2450 K. At 2550 K and higher temperatures, the density profile exhibits a flat profile indicating clearly that the phase transition has been accomplished.

An interesting feature observed in Fig. 4 is the two prominent peaks observed at 1900 K. As shown in Fig. 5, where partial density profiles are reported, these peaks are due to a second layer of Cr atoms. According to the well-known corundum distortions, the Cr layers are split as shown in Fig.

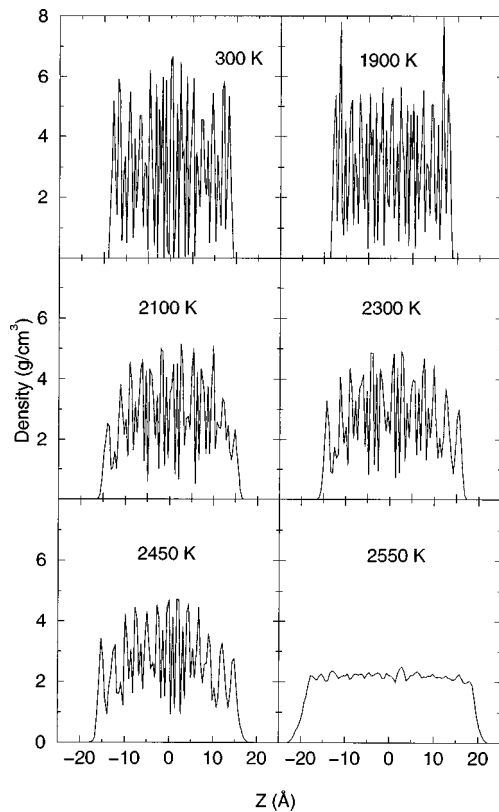


FIG. 4. Averaged total density profiles of the system along the  $c$  axis as a function of temperature.

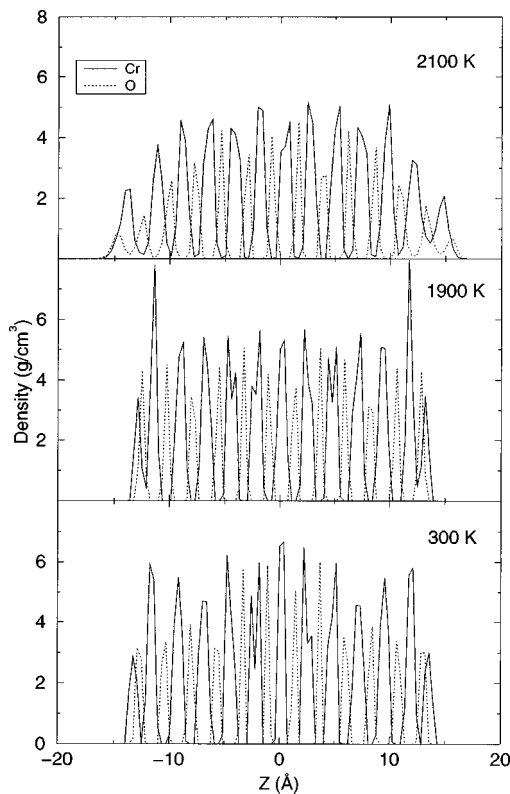


FIG. 5. Averaged partial density profiles of the system along the  $c$  axis at 300, 1900, and 2100 K.

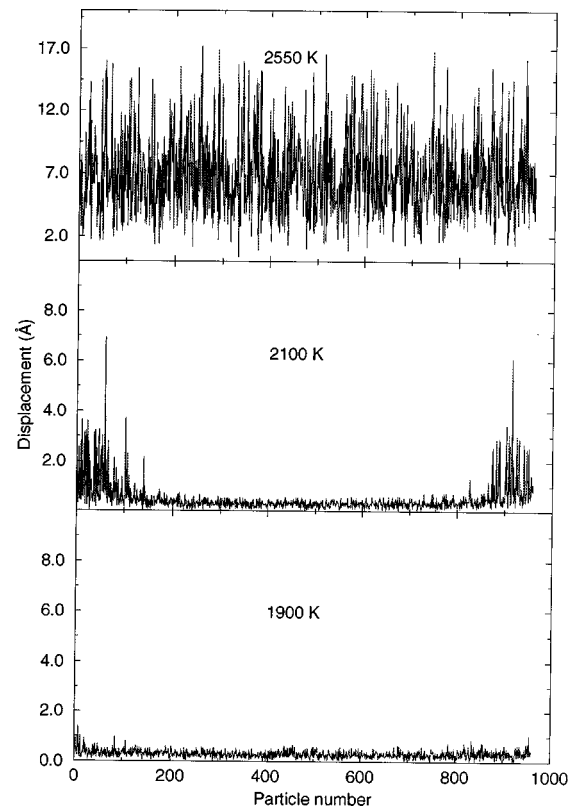


FIG. 6. Relative displacement of all particles, with respect to their original positions after 100 ps of simulated time at 1900, 2100, and 2550 K. Lower and higher indices correspond to superficial particles, whereas medium indices correspond to particles in the medium layers.

1(b). However, because of surface relaxation, such a split is lower for surface layers and decreases when temperature rises. At 1900 K, the second-layer Cr atoms are virtually at the same depth, originating those sharp, more intense peaks. The fact that these Cr atoms are located, in an averaged way, at the same  $z$  coordinate, involves a larger Coulombic repulsion, and when they reach enough kinetic energy, they can jump to the surface giving rise to local defects which are the origin of the surface melting.

Figure 6 shows the total displacement, after 100 ps simulation, versus particle number as a function of temperature. Particles were numbered from  $-c$  to  $c$  in ascending order. Therefore the extremes of the plots represent the outermost layers. In the lower panel of the figure, where temperature is 1900 K, the total displacement corresponds to the result of the normal vibrations of particles. In the middle panel (2100 K) the premelting is evident from the relatively large displacement of particles in the outermost layers comprised in approximately the final 4 Å, these corresponding to three layers. In the uppermost panel, where the system is at 2550 K, the system appears totally liquid.

The premelting process also appears clearly by analyzing the partial radial distribution functions  $g(r_{\text{Cr-Cr}})$ ,  $g(r_{\text{Cr-O}})$ , and  $g(r_{\text{O-O}})$ , calculated over the whole slab. These functions are plotted in Fig. 7 at 300, 2450, and 2550 K. At 300 K (lower panel) the peaks are sharp and well defined, and appear at the correct experimental distances as shown in Table IV, where the corresponding experimental values are also included.<sup>19</sup> In this table the distance  $r_{\text{CrO}}$  of 1.81 Å corresponds to the

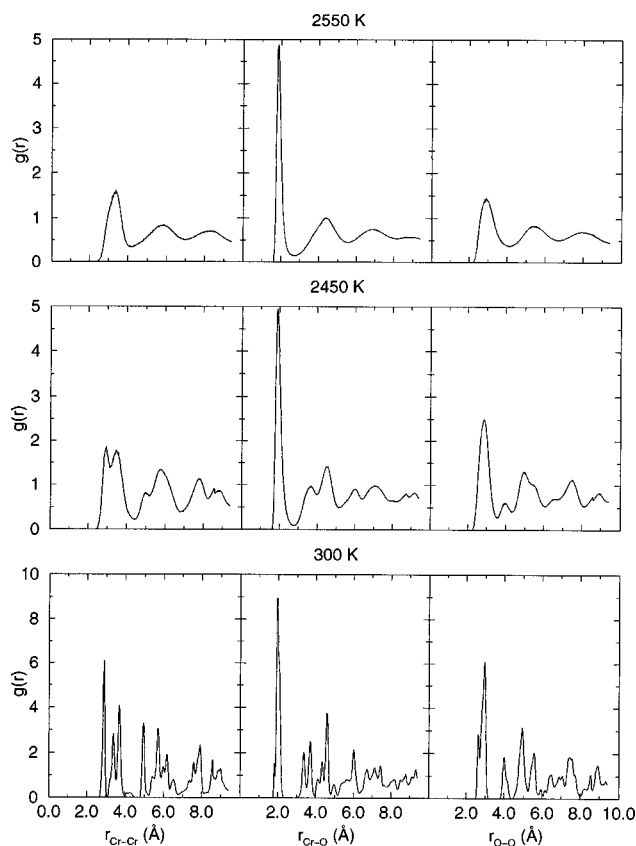


FIG. 7. Partial radial distribution functions  $g(r_{\text{CrCr}})$ ,  $g(r_{\text{CrO}})$ , and  $g(r_{\text{OO}})$  at 300, 2450, and 2550 K.

threefold coordinated chromium atoms at the terminating layers. On the other, at 2550 K, top panel of Fig. 7, the radial distribution functions are broad in agreement with the fact that the system is totally liquid. Moreover, it is observed that the curves do not tend to unity, as expected for a liquid, this feature being due to the volume change occurring when the system melts (see last snapshot in Fig. 3). However, at 2450 K, middle panel, the shapes exhibited by the curves are found to be intermediate between the crystal and liquid ones. With respect to the crystalline situation, there is a loss of resolution and the first-neighbor peak does not reach the zero, while with respect to the liquid state, the better resolution reflects a more ordered structure of the system.

In order to look at the motion of atoms in a detailed way, we have calculated the diffusion coefficients of both oxygen

TABLE IV. Positions of the first five peaks of the calculated radial distribution functions and corresponding experimental data.

Cr-Cr		Cr-O		O-O	
Expt.	MD	Expt. <sup>a</sup>	MD	Expt.	MD
2.89	2.89	1.96	1.81, <sup>b</sup> 1.95	2.62	2.62
3.42	3.38	2.01	2.02	2.73	2.74
3.64	3.68	3.37	3.37	2.84	2.84
4.95	4.95	3.63	3.71	2.99	2.96
5.35	5.43	3.69	3.71	3.95	3.99

<sup>a</sup>Reference 19.

<sup>b</sup>This value corresponds to superficial Cr atoms.

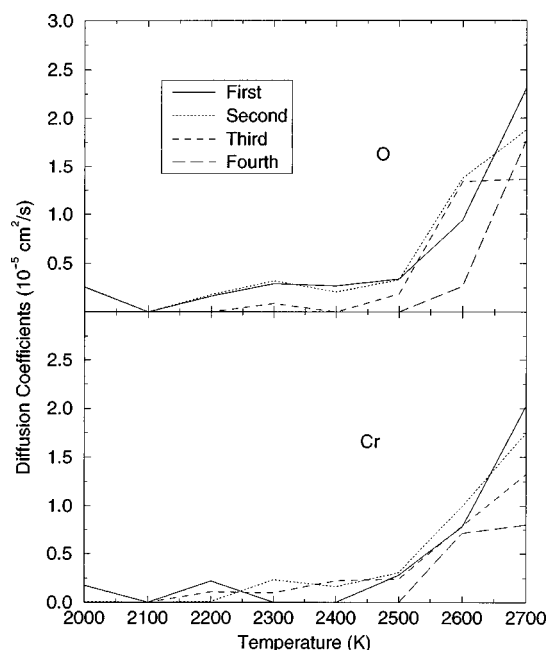


FIG. 8. Calculated diffusion coefficients for oxygen and chromium atoms of the first four layers as a function of temperature.

and chromium species of the first four layers<sup>20</sup> separately as a function of temperature using Einstein's relation<sup>16</sup>

$$D = \lim_{t \rightarrow \infty} \frac{\langle \sum_i |\mathbf{r}_i(t) - \mathbf{r}_i(0)|^2 \rangle}{6t}$$

The results for the range [2000–2800] K are shown in Fig. 8. In the upper panel it is shown that the first and second layers of oxygen atoms start diffusing almost at the same rate. The oxygens located in the third and fourth layers start diffusing at higher temperatures, namely 2500 K in the third and 2600 K in the fourth. This happens because the uppermost layer is of chromium atoms, which, as can be seen from the lower panel of Fig. 8, start diffusing at 2200 K. These layers of Cr atoms are bonded to the first layer of oxygens and therefore drag them during the diffusing process. However, around 2300 K the diffusion coefficient of Cr atoms drops because the second layer of oxygen atoms also starts moving and prevents the upper layers from moving further. When kinetic energy is large enough to let the uppermost layer of chromium atoms move, between 2400 and 2450 K, the third and fourth layers of oxygens start diffusing. In other words, the upper layers seem to acquire a partially disordered configuration allowing light atoms, such as oxygens, to move inside superficial channels formed by the heavier chromium atoms.

In order to investigate whether the diffusion mechanism of a given species is by hopping or like in a liquid, the ratio of the fourth moment of the displacement to the second moment of the mean-square displacement,  $P_\alpha$ , was computed through the expression

$$P_\alpha(t) = \frac{3\langle [\Delta \mathbf{r}(t)]_\alpha^4 \rangle}{5\langle [\Delta \mathbf{r}(t)]_\alpha^2 \rangle^2} = 1.$$

$P_\alpha = 1$  indicates that particles of the system have a harmonic motion or that the system is in liquid state. In terms of diffusion this implies that there is no diffusion at all or else the

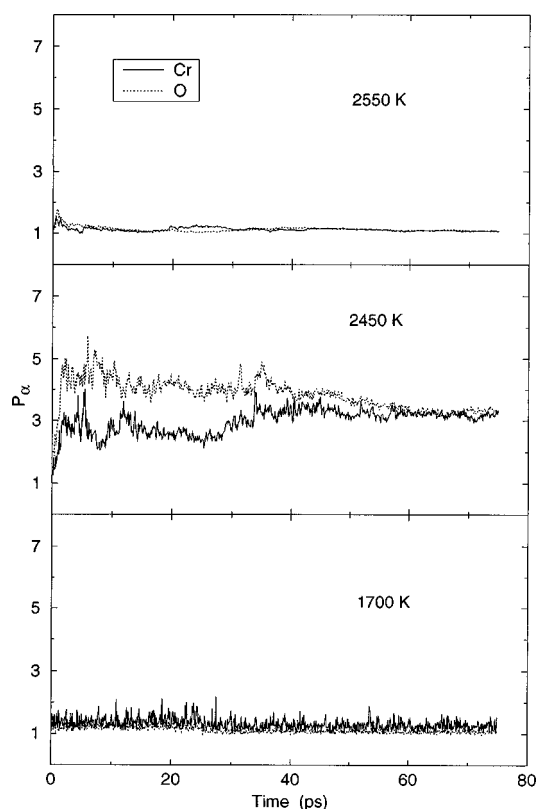


FIG. 9. Plots of  $P_\alpha$  versus time for the simulated system at 1700, 2450, and 2550 K.

diffusion mechanism is like in a liquid. If  $P_\alpha \neq 1$  then the mechanism is by hopping. Figure 9 shows plots of  $P_\alpha$  versus time for the simulated system at 1700, 2450, and 2550 K. At 1700 K there is no diffusion as stated above, and  $P_\alpha$  oscillates around unity, indicating a harmonic motion of all particles, that is to say,  $P_\alpha$  reflects the thermal vibration of particles. At 2450 K both the chromium and oxygen curves

present a clearly nonharmonic motion, indicating that the mechanism of diffusion is indeed by hopping from one relatively stable site to another. The oxygen curve has larger values of  $P_\alpha$ , and shows a certain correlation to the chromium curve. This seems to confirm what we stated above related to the drag of oxygen layers by superficial chromium atoms. Finally, at 2550 K the values of  $P_\alpha$  lose the noise and flatten around a constant value near unity, indicating that the diffusion process is already that of a liquid system.

#### IV. CONCLUSIONS

MD simulations of the surface of  $\text{Cr}_2\text{O}_3$  have been carried out using two different potential functions. The descriptions of the structural properties of the system are similar in both cases and are in agreement with experimental data. However only the Pauling-type function is able to reproduce the experimental melting point, the error being less than 0.02%. The analysis of density profiles, atomic displacements, radial distribution functions, and diffusion coefficients indicates that a surface melting occurs at temperatures well below the melting point. Our simulations show that this process starts at 2000 K when some chromium atoms jump from the second layer to the surface, inducing a disorder. The diffusion mechanism of the atoms in such a disordered surface is found to be hopping.

#### ACKNOWLEDGMENTS

This work was partially supported by Cray Research Inc. through supercomputing Grant No. Cray-UNAM, DGAPASC-2095, Proyecto V.4 of Programa Iberoamericano de Ciencia y Tecnología para el Desarrollo (CYTED) and Comisión Interministerial de Ciencia y Tecnología (MAT97-0717, PB95-1247). M.A.S. also thanks the Ministerio de Educación y Ciencia of the Spanish Government for the award of an FPI grant.

\*Author to whom correspondence should be addressed. Electronic address: smiguel@cica.es

<sup>1</sup>L. Vocadlo and G. D. Price, *Phys. Chem. Miner.* **23**, 42 (1996), and references therein.

<sup>2</sup>H. Häkkinen and M. Manninen, *Phys. Rev. B* **46**, 1725 (1992).

<sup>3</sup>P. M. Oliver, G. W. Watson, and S. C. Parker, *Phys. Rev. B* **52**, 5323 (1995).

<sup>4</sup>G. Ciccotti, M. Guillopé, and V. Pontikis, *Phys. Rev. B* **27**, 5576 (1983).

<sup>5</sup>E. T. Chen, R. N. Barnett, and U. Landman, *Phys. Rev. B* **41**, 439 (1990).

<sup>6</sup>P. Stoltze, J. K. Nørskov, and U. Landman, *Phys. Rev. Lett.* **61**, 440 (1988).

<sup>7</sup>P. Carnevali, F. Ercolessi, and E. Tosatti, *Phys. Rev. B* **36**, 6701 (1987).

<sup>8</sup>P. J. Lawrence, Ph.D. thesis, School of Chemistry, University of Bath, UK, 1989.

<sup>9</sup>M. Cati, G. Sandrone, G. Valerio, and R. Dovesi, *J. Phys. Chem. Solids* **57**, 1735 (1996).

<sup>10</sup>R. D. Shannon and C. T. Prewitt, *Acta Crystallogr., Sect. B: Struct. Crystallogr. Cryst. Chem.* **B25**, 925 (1969).

<sup>11</sup>D. J. Adams and I. R. McDonald, *Physica (Amsterdam)* **B79**, 159 (1970).

<sup>12</sup>G. V. Lewis and C. R. A. Catlow, *J. Phys. C* **18**, 1149 (1985).

<sup>13</sup>R. Ferneyhough, D. Fincham, G. D. Price, and M. J. Gillan, *Modell. Simul. Mater. Sci. Eng.* **2**, 1101 (1994).

<sup>14</sup>D. Fincham, W. C. Mackrodt, and P. J. Mitchell, *J. Phys.: Condens. Matter* **6**, 393 (1994).

<sup>15</sup>SIMULA is a molecular-dynamics and visualization software developed by L. J. Álvarez and M. A. San Miguel, Universidad Nacional Autónoma de México, 1995.

<sup>16</sup>M. P. Allen and D. J. Tildesley, *Computer Simulation of Liquids* (Clarendon, Oxford, 1987).

<sup>17</sup>R. Rohr, M. Bäumer, H.-J. Freund, J. A. Mejías, V. Staemmler, S. Müller, L. Hammer, and K. Heinz, *Surf. Sci.* **372**, L291 (1997).

<sup>18</sup>C. Rehbein, N. M. Harrison, and A. Wander, *Phys. Rev. B* **54**, 14 066 (1996).

<sup>19</sup>L. W. Finger and R. M. Hazen, *J. Appl. Phys.* **51**, 5362 (1980).

<sup>20</sup>The atoms were identified as belonging to a given layer according to the initial corundum structure, and this labeling was maintained during the simulations.